Appl. Phys. A 66, S27–S30 (1998)

Applied Physics A
Materials
Science & Processing

Applications with a new low-temperature UHV STM at 5 K

T. Becker[1], **H. Hövel**[2,*], **M. Tschudy**[2], **B. Reihl**[2,*]

[1] OMICRON Vakuumphysik GmbH, D-65232 Taunusstein, Germany
[2] IBM Zurich Research Laboratory, CH-8803 Rüschlikon, Switzerland

Received: 25 July 1997/Accepted: 1 October 1997

Abstract. A new dedicated UHV STM for investigations at $T \leq 5\,\mathrm{K}$ is presented. To achieve such low temperatures and to ensure a high thermal stability, the low-temperature (LT) STM described here has a concentric system of bath cryostats. There are openings for tip and sample exchange at low T, and windows with an infrared radiation shield for optical access, which can both be closed by a door mechanism for LT-STM measurements. Efficient vibration isolation is realized by using spring suspension with eddy current damping. With the 3-d coarse positioning unit any region of interest within 5 mm by 5 mm on the sample is accessible even at 5 K. For short turn-around cycles the sample and tip can both be exchanged at low temperatures. Atomically resolved images of Au(111) at 5 K in UHV demonstrate the excellent performance of this LT STM. As a typical application example the appearance of a charge-density wave on $NbSe_2$, which occurs below a transition temperature of 33.5 K, was imaged.

In surface and interface science T-dependent bulk phenomena like magnetism or superconductivity persist, but the surface acts as a "disturbance" with new or different T-dependencies. In addition, new T-dependent effects exist at interfaces or on surfaces: surface reconstruction, growth mechanisms (cluster formation, island growth, stability and size effects), surface metallization, gas adsorption, etc. Since changes in temperature often enter through an exponential of $(\pm k_\mathrm{B}T)$ or T^n power dependence, temperature phenomena get strongly enhanced.

Scanning tunneling microscopy (STM) is well suited to study of both the geometric and electronic properties of surfaces as well as their interdependencies. Due to its scanning action, however, STM is a relatively slow probe. By cooling, phenomena like diffusion and corrosion can sufficiently be slowed down so that they become accessible by scanning probe techniques. Since vibrational and rotational movements of single atoms and molecules are also frozen in with cooling, STM topographic pictures often appear crisper at lower T. In cases where the signal-to-noise ratio is poor in an STM experiment (like in STM-induced photon emission [1], or electron emission [2]), increasing the tunneling current can often help. This, however, is limited by thermal heating and eventually destroys the STM tip. Typical maximum tunneling currents are $I_\mathrm{t} \cong 100\,\mathrm{nA}$ for a tungsten tip. At low temperature ($T \leq 10\,\mathrm{K}$) tunneling currents reach well into the μA range, hence improving signals which are proportional to it.

There have been several attempts to develop low-temperature STM. In the first successful designs, the whole STM was immersed in liquid helium or cold helium gas. The movement of the vortex in superconducting $NbSe_2$ was imaged in this way [3]. However, in cases where the sample is not as inert as, e.g., $NbSe_2$ complications in the interpretation of STM images may arise owing to a contamination of the sample surface and/or tip when working at ambient pressures. The best characterized environment for STM is ultra-high vacuum (UHV) also at low temperatures. Eigler and Schweizer [4] were the first to optimize this goal and set the standards of this novel STM field. Their rather rigid design achieves a very high thermal stability with essentially no drift over periods of days, but at the expense of flexibility in sample and tip handling, resulting in rather long turn-around times. Manipulation of single xenon atoms on Ni(110) at 4 K and the visualization of the standing electron waves of a surface state on Cu(111) are just two examples of Eigler et al.'s spectacular results [4, 5].

A first successful set-up of a low-temperature UHV STM with the full in-situ flexibility of tip and sample exchange at 5 K was realized at the IBM Zurich Research Laboratory [6]. Ordered overlayers of C_{60} on the Au(110) surface could be visualized [7] together with some internal structures of single C_{60} molecules in different adsorption orientations and corresponding STM-induced photon-emission maps [8]. Experience showed, however, that certain improvements of that design [6] would greatly enhance the performance of the UHV STM at low temperatures.

1 Experimental

A key requirement (besides an operating pressure in the 10^{-11} mbar range and temperatures down to 5 K) is the possibility to remove the sample holder and tip in situ for sam-

* *Present address*: University of Dortmund, Experimentelle Physik I, D-44221 Dortmund, Germany; Homepage: http://e1.physik.uni-dortmund.de

ple preparation and characterization, without warming up the cryostat. This flexibility together with the boiling liquid nitrogen and helium put severe constraints on the vibrational damping of the design. In the following we describe the new LT STM solution which was developed in a joint effort of OMICRON Vakuumphysik GmbH and the IBM Zurich Research Laboratory, and present first application examples of atomically resolved surface structures: Au(111) on Mica, Si(111) 7×7, charge-density waves on $NbSe_2$(111), and a nanopit in graphite for the formation of metal clusters.

The apparatus containing the new LT STM consists of a custom-designed cryostat chamber and a preparation chamber connected by an Omniax *x-y-z* sample translator [9] with fast-load lock for sample introduction. A custom-built LHe flow cryostat provides cooling capabilities to the sample translator with full 360° of rotation. The two main chambers are pumped by ion-getter and Ti-sublimation pumps to base pressures in the 10^{-11} mbar range. The cryostat chamber contains the liquid-helium (LHe) bath cryostat surrounded by a liquid-nitrogen (LN_2) dewar (see Fig. 1). In the preparation chamber, tips and samples can be heated and sputter-cleaned as well as be exposed to various evaporation sources and gases. They can then be put inside a storage carousel in the cryostat chamber, which is cooled to LN_2 temperatures. On the sample translator tip and sample can be cooled to 40 K prior to their insertion into the STM head. This novel concept is the key to the very short turn-around times of less than 1 hour, before thermal equilibrium is reached and drift effects in the STM get below 0.2 nm/hour.

A schematic of the cryogenic section is shown in Fig. 1 with the LHe dewar (1) and a cross-section of the LN_2 dewar (2) surrounding the helium dewar. Both cryostats are mounted on CF flanges and get filled from above. They are independently elongated at their respective bottoms by concentric copper cylinders (3) with door mechanisms (not shown in Fig. 1) for tip/sample exchange and infrared-filter windows for optical access. The STM block (4) is hanging down from 3 springs (5), each of which is running within a tube (6) through the LHe dewar and is mounted to the top of the LHe cryostat. During cool-down a pull-up mechanism employing 3 stainless-steel wires running through the suspension springs (not shown in Fig. 1) allows to firmly press the STM body against the bottom of the LHe dewar. In this position tip and sample can be exchanged by a wobble-stick which reaches into the copper containers, after their doors have been opened. When the minimum temperature has been reached, the pull-up mechanism is relaxed and the whole STM body lowered by about 5 mm to hang freely from the springs. The bottom plate on which the whole STM body is mounted has copper wings which radially stick into a concentric periodic magnet structure for eddy-current damping.

The schematics of the STM itself are also shown in Fig. 1. Its sample stage is made form a copper block and designed to ensure a good thermal coupling of the whole stage and the sample. Since the whole STM is placed within the copper housing which is at 4.2 K, a uniform temperature distribution is achieved resulting in a very low STM drift rate, measured to be less than 0.2 nm/hour (see Applications below). The scanner is mounted on the 3-axis piezo coarse motor (range: 5 mm × 5 mm × 10 mm) by employing OMICRON's micro piezo slide principle [10]. The scan range of the tube scanner [11] is temperature dependent with values of 10 μm, 4.4 μm, and 1.8 μm at 300, 77, and 4.2 K, respectively. The tip itself is magnetically attached to the top of the scanner, while the sample is pushed in horizontally from the front, with the sample surface facing the tip upside down. The preamplifier (amplification 2×10^9) is directly attached to the UHV feedthrough on the top flange of the cryostat to minimize the length of the cable for the tunneling current.

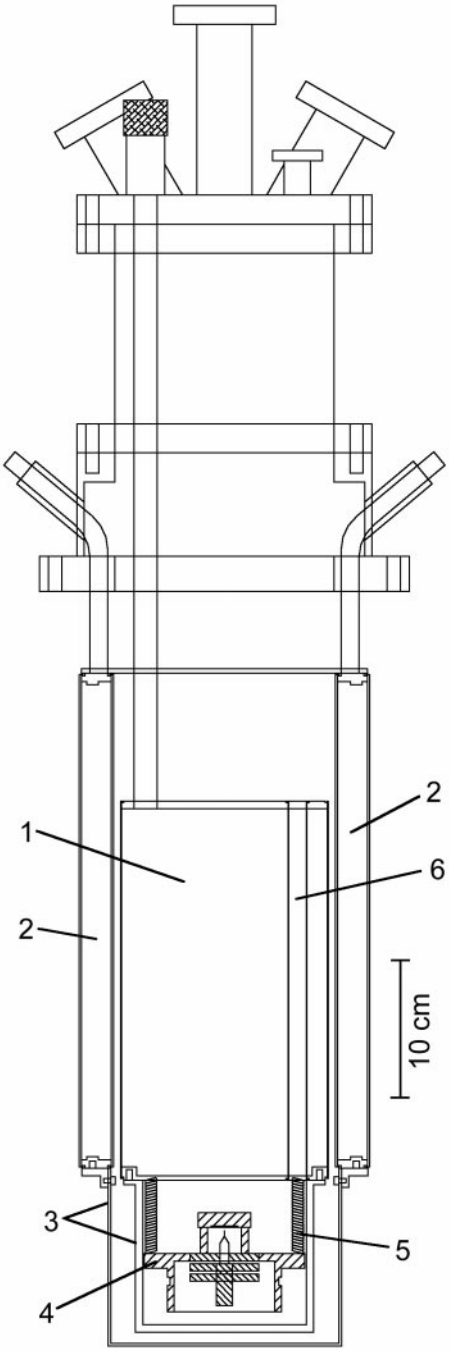

Fig. 1. Schematic of the cryogenic set-up of the LT STM with the STM body hanging in its concentric copper housings at the bottom of the cryostat: (1) LHe dewar, (2) LN_2 dewar, (3) concentric copper cylinders with doors and windows, (4) STM block, (5) three springs, and (6) tubes for springs. Not shown are the door mechanisms and the stainless steel wires to firmly pull up the STM body and press it against the bottom of the LHe dewar for cooling down or tip and sample exchange

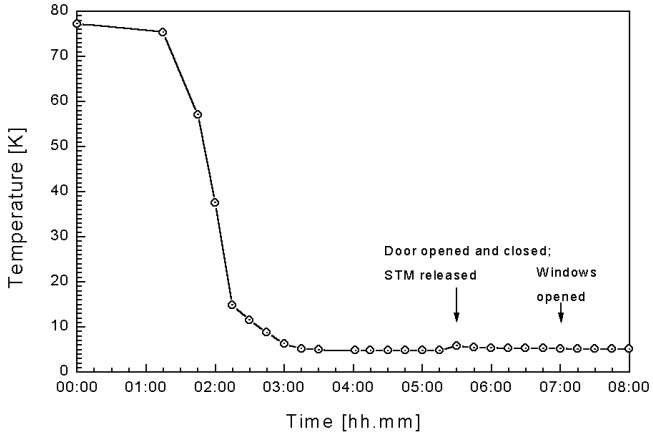

Fig. 2. Temperature measured near the position of the sample as a function of time during cooling down from 77 K (LN_2 temperature) to 5 K. Note the slight increase in T when the door is opened for several minutes. No temperature rise is observed, however, when opening the infrared-shielded windows

A temperature sensor is mounted near the position of the sample. The wires for the STM and the T sensors are running from the top flange along the helium exhaust tubes, where they are anchored, along the LHe cryostat chamber and are glued into a cooling mount at its bottom to ensure a proper pre-cooling to 4.2 K. A typical cool-down cycle (temperature versus time) is shown in Fig. 2, starting from 77 K, the LN_2 temperature, which is being reached after 2 hours, resulting in a total 300 K-to-5 K cool-down time of less than 5 hours. After reaching 5 K, the whole STM body is released from its cool-down position (pressed against the bottom of the LHe dewar) to hang freely but damped within the copper housings. Opening the doors increases the temperature immediately as can be seen in Fig. 2, while opening the infrared-shielded windows has no effect. Resistive heating within the STM housing allows the temperature to be stabilized in the range $5\,\mathrm{K} < T < 60\,\mathrm{K}$. One 4-liter filling of the LHe dewar lasts for more than 16 hours before a refill is necessary.

In summary, the novel LT STM described here has the following major new features: 3-dimensional x-y-z coarse approach which allows any point on the sample surface to be reached within a $5\,\mathrm{mm} \times 5\,\mathrm{mm}$ square; vibrational isolation via spring suspension and eddy-current damping, which makes the freezing of the liquid nitrogen obsolete and prevents acoustic and mechanical vibrations from coupling in; faster cooling down from 300 K to 5 K in less than 5 hours; faster tip and sample exchange at 5 K with thermal equilibrium conditions reached again after less than 1 hour; part of a system solution with standardized surface-science techniques as simple attachments; temperature measurement near the sample-tip region; sample heating and temperature stabilization in the range $5\,\mathrm{K} < T < 60\,\mathrm{K}$.

2 Applications

Gold evaporated on Mica and thermally annealed produces a well-ordered (111) surface with a $23 \times \sqrt{3}$ reconstruction [12]. An STM topographic image from a surface with such a small corrugation of $\Delta z = 0.02\,\mathrm{nm}$ is a very stringent test of the performance of the STM and the efficiency of the vibrational damping. In Fig. 3 we show an Au(111) image measured at 5 K with atomically resolved structures and the typical stripes of the $23 \times \sqrt{3}$ surface reconstruction. Near the front corner of this pseudo-3D image a ring-like structure can be seen, which we attribute to an adsorbate located in the center of the ring, but which is invisible at this tunneling voltage.

The Au(111) $23 \times \sqrt{3}$ reconstructed surface with atoms separated by 0.288 nm is also used for the calibration of the piezos at the various temperatures and in particular at 5 K.

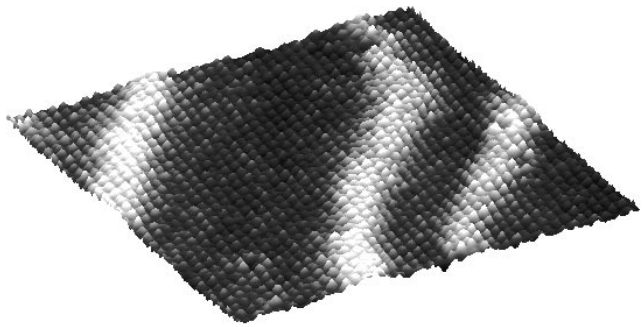

Fig. 3. Pseudo 3D image of the Au(111) surface with atomic resolution at 5 K ($V_t = 0.07$ V, $I_t = 3.74$ nA, scan area $10\,\mathrm{nm} \times 10\,\mathrm{nm}$). The stripes reflect the $23 \times \sqrt{3}$ surface reconstruction. This figure represents the topographic raw data with a background correction and a smoothing of four-next-neighbor pixels

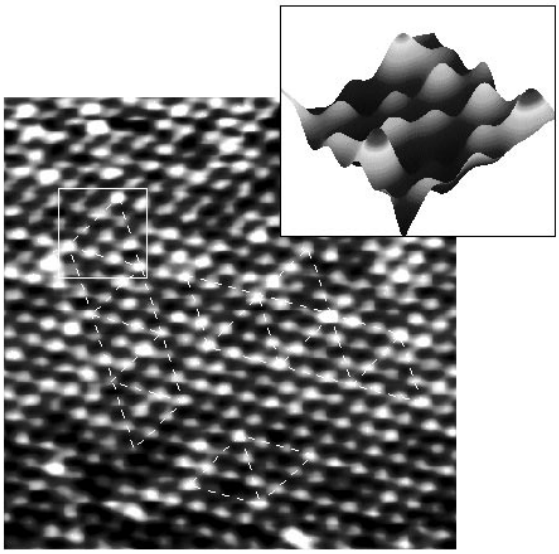

Fig. 4. Top view image of the $NbSe_2$(111) at 5 K surface with atomic resolution. Clearly visible are the three domains of the charge-density wave (*dashed lines*). A pseudo-3D image of the square section is shown as an inset. Parameters: $V_t = 0.02$ V, $I_t = 2.55$ nA, scan area $5\,\mathrm{nm} \times 5\,\mathrm{nm}$. The STM data for this figure were low-pass filtered in the Fourier transformation

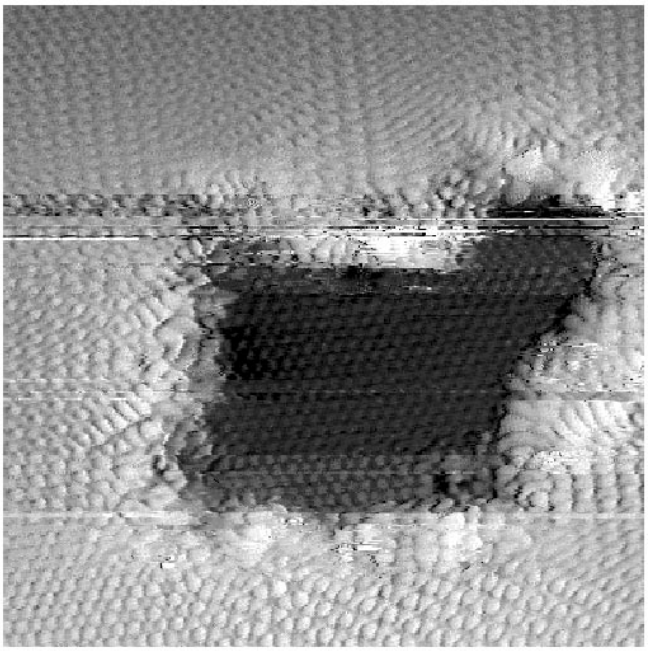

Fig. 5. A typical nanopit produced in the HOPG surface imaged at 5 K. Note the atomic resolution also at the bottom of the pit. Parameters: $V_t = 0.10$ V, $I_t = 0.69$ nA, scan area $10.4\,\text{nm} \times 10.4\,\text{nm}$. The STM data were differentiated to enhance the grey-scale contrast on the atomic level

The Si(111) 7×7 reconstructed surface was measured at $T = 5$ K and revealed a nicely resolved atomic structure in agreement with the literature [13] with the 12 adatoms per unit cell and the typical corner holes (STM topographic images not shown here). Single defects, i.e. missing adatoms, at fixed positions allowed to identify and observe the same scan area over a period of several hours, and hence determine the temperature drift of the STM at 5 K, yielding 0.2 nm/hour as the maximum drift.

Charge-density waves (CDW) on $NbSe_2(111)$ are difficult to observe by STM [14], because the long-range coupling responsible for the CDW pattern is very weak. As a consequence regular patterns are usually only found in small surface areas and are often split into different phase domains. Furthermore, the corrugation amplitude is relatively small ($\cong 0.02$ nm). The image shown in Fig. 4 was acquired at $T = 5$ K, i.e. about 28.5 K below the CDW transition temperature of 33.5 K. Different domains of the incommensurate CDW with a wavelength of $\lambda_{CDW} \approx 3\,a_0$ are clearly visible.

By sputtering and subsequent heating in on oxygen atmosphere, well-defined nanopits can be generated on HOPG (graphite) surfaces [15], which may serve as coagulation centers for the growth of metal clusters. The goal is then to measure their properties as a function of size and particle number. Only at low temperatures was it possible to resolve atomic structures also at the bottom of these pits, i.e. in the second layer of graphite and hence prove that the nanopit was etched to only one atomic layer deep, and that the second graphite layer was defect-free. Such an example measured with the LT STM at 5 K is shown in Fig. 5.

3 Conclusions

The novel LT STM working in UHV with in-situ tip and sample exchange and very short cool-down and turn-around cycles provides atomically resolved STM pictures of metals and semiconductors with thermal drifts below 0.2 nm/hour.

Acknowledgements. We thank H. Rohrer for his continuous support during the course of this project development. H.H. acknowledges the support by the Feodor Lynen Program of the Alexander von Humboldt Foundation.

References

1. J.K. Gimzewski, B. Reihl, J.H. Coombs, R.R. Schlitter: Z. Phys. B **72**, 497 (1988);
   J.H. Coombs, J.K. Gimzewski, B. Reihl, J.K. Sass, R.R. Schlitter: J. Microsc. **152**, 325 (1988)
2. B. Reihl, J.K. Gimzewski: Surf. Sci. **189**/**190**, 36 (1987)
3. H.F. Hess, R.B. Robinson, R.C. Dynes, J.M. Valles, Jr., J.V. Waszcak: Phys. Rev. Lett. **62**, 214 (1989)
4. D.M. Eigler, E.K. Schweizer: Nature **344**, 524 (1990)
5. M.F. Crommie, C.P. Lutz, D.M. Eigler: Nature **363**, 524 (1993)
6. R. Gaisch, J.K. Gimzewski, B. Reihl, R.R. Schlittler, M. Tschudy, W.D. Schneider: Ultramicroscopy **42**–**44**, 1621 (1992)
7. R. Gaisch, R. Berndt, J.K. Gimzewski, B. Reihl, R.R. Schlittler, W.D. Schneider, M. Tschudy: Appl. Phys. A **57**, 381 (1993)
8. R. Berndt, R. Gaisch, J.K. Gimzewski, B. Reihl, R.R. Schlittler, W.D. Schneider, M. Tschudy: Science **262**, 1425 (1993)
9. Vacuum Generators, Hastings, England
10. OMICRON Micro Piezo Slide, US Patent No. 5,237,238; D Patent Nr. 40 23 311
11. Tube scanner: 3/4 inch long, PZT 5A with a sensitivity of 171×10^{-12} m/V at 300 K and 31×10^{-12} m/V at 4.2 K
12. U. Harten, A.M. Lahee, J.P. Toennies, Ch. Wöll: Phys. Rev. Lett. **54**, 2619 (1985);
    Ch. Wöll, S. Chiang, R.J. Wilson, P.H. Lippel: Phys. Rev. B **39**, 7988 (1989)
13. R.M. Tromp, R.J. Hamers, J.E. Demuth: Phys. Rev. B **34**, 1388 (1986)
14. R.V. Colema, B. Giambattista, P.K. Hansma, A. Johnson, W.W. McNairy, C.G. Slongh: Adv. Phys. **37**, 559 (1988)
15. H. Hövel, Th. Becker, A. Bettac, B. Reihl, M. Tschudy, E.J. Williams: J. Appl. Phys. **81**, 154 (1997)